SANDIA REPORT

SAND2015-8118
Unlimited Release
September 2015

Pre-Compressed Targets for Gas Gun Studies

Christopher T. Seagle, Andrew J. Lopez

Prepared by
Sandia National Laboratories
Albuquerque, New Mexico 87185 and Livermore, California 94550

Sandia National Laboratories is a multi-program laboratory managed and operated by Sandia Corporation, a wholly owned subsidiary of Lockheed Martin Corporation, for the U.S. Department of Energy's National Nuclear Security Administration under contract DE-AC04-94AL85000.

Issued by Sandia National Laboratories, operated for the United States Department of Energy by Sandia Corporation.

Available to DOE and DOE contractors from
U.S. Department of Energy
Office of Scientific and Technical Information
P.O. Box 62
Oak Ridge, TN 37831

Telephone: (865) 576-8401
Facsimile: (865) 576-5728
E-Mail: reports@osti.gov
Online ordering: http://www.osti.gov/scitech

Available to the public from
U.S. Department of Commerce
National Technical Information Service
5301 Shawnee Rd
Alexandria, VA 22312

Telephone: (800) 553-6847
Facsimile: (703) 605-6900
E-Mail: orders@ntis.gov
Online order: http://www.ntis.gov/search

SAND2015-8118
Unlimited Release
September 2015

Pre-Compressed Targets for Gas Gun Studies

Christopher T. Seagle, Andrew J. Lopez
Sandia National Laboratories
P.O. Box 5800
Albuquerque, New Mexico 87185-MS1189

Abstract

This work developed the capability for pre-compressing targets for Hugoniot measurements utilizing gas gun driven flyer plates. Initial condition control, such as pre-compression, allows access to states off the principal Hugoniot and in the case of highly compressible materials, the locus of shock states may be well off (significantly denser than) the principal Hugoniot even for relatively modest (~100's MPa) initial pressures. The design and operation of the pre-compression target hardware will be discussed in relation to functionality and design considerations for dynamic testing. Capability for loading of super critical gases and gas mixtures has been successfully demonstrated and dynamic hypervelocity impacts of helium were tested. Example loading of supercritical alcohol (ethanol) will is presented in the context of previous impact studies of initially ambient quiescent liquid. Advantages and limitations of the system are discussed in the context accessing highly compressed states.

ACKNOWLEDGMENTS

Many individuals contributed to this project.

- Andrew Lopez did much of the design and drafting work for hardware, as well as significant amounts of safety calculations and paperwork for the gas loading system
- Nicole Cofer prepared ruby/sapphire stacks and provided metrology data
- Josh Usher helped to load gasses with the gas loading system
- Aaron Bowers, Keith Hodge, Randy Hickman, Nicole Cofer and Jesse Lynch operated the DICE gas gun and associated diagnostics
- Richard Hacking and Sherri Payne helped design and field diagnostics
- Bill Reinhart, Tom Thornhill, John Martinez, and Robert Palamino operated the STAR 2-stage light gas gun and diagnostics
- Dan Dolan provided advise and the “Romulan” probes used for the STAR_3 shot
- Center 1830 developed the method for depositing the “donut” coatings used

CONTENTS

FIGURES

TABLES

NOMENCLATURE

DICE	Dynamic Integrated Compression Experiments facility
EoS	Equation of State
GPa	Giga-Pascal
LDRD	Laboratory Directed Research and Development
MPa	Mega-Pascal
PDV	Photonic Doppler Velocimetry
STAR	Shock Thermodynamics Applied Research facility
VISAR	Velocity Interferometer System for Any Reflector
WC	Tungsten Carbide
PH	Precipitation Hardened (Steel)
2SLGG	2-Stage Light Gas Gun

1. INTRODUCTION

Plate impact shock experiments probe a single state on the Hugoniot, defined as the locus of shock states for a material. The principal Hugoniot, which is unique to each material, is a set of pressure (P), temperature (T) points in phase space. Real world dynamic loading phenomena are often not a well-controlled uniaxial plate impact type of configuration and as a result, material trajectories through phase space may explore regions not accessible to standard gas gun experiments. Initial condition control of the sample is one way of achieving access to states off the principal Hugoniot. A number of researchers have developed techniques for producing porous samples. This introduces additional shock heating due to collapse of the pores and results in a higher temperature, lower density end state on shock compression [1]. Similarly, pre-heating targets also ends in a higher temperature, lower density state [2]. Shock-release techniques likewise probe this low density side of the Hugoniot by interrogating the isentropic release of the material from the shocked state [3]. In the past it has been significantly more challenging to access the phase space region at densities higher than the Hugoniot density (at constant T). This region can be accessed with double-shock experiments [4], shockless compression [5], shock-ramp techniques [6] or through initial condition control of the pressure [7].

The focus of LDRD 165739, begun in FY2013 and ended in FY2015, was to develop the capability for pre-compressing targets large enough for gas gun studies. For pre-compression to actually be beneficial for the purpose of probing states denser than the Hugoniot, a minimum initial pressure must be applied to the sample. The magnitude of this pressure will depend on the compressibility of the sample of interest, but in general higher initial pressures will be required for more highly incompressible materials. For this reason, and the difficulty associated with achieving large static pressures on macroscopic samples, this LDRD focused on pre-compressing fluids where small static pressures have a large effect on the end shock states relative to ambient fluid. The following characteristics are required for pre-compression gas gun targets.

1. Sample diameters must be larger than 2.5 mm.

2. Sample pressures must be greater than 200 MPa.

3. Sample stack thicknesses must be less than 2.5 mm.

These characteristics will typically assure avoidance of edge waves and maintenance of one dimensional uniaxial compression at the center of the sample. The initial pressure will also, at least for fluids, result in a locus of shock states experimentally distinguishable from the principal Hugoniot.

1.1. Benefits of Pre-Compression

For a given flyer plate velocity, pre-compression results in a higher density shock state and allows regions of phase space between the principal isentrope and principal Hugoniot to be probed. Figure 1 shows a calculation of the Hugoniot for neon starting at different initial

pressures. Neon is highly compressible; even moderate initial pressures significantly increase the density.

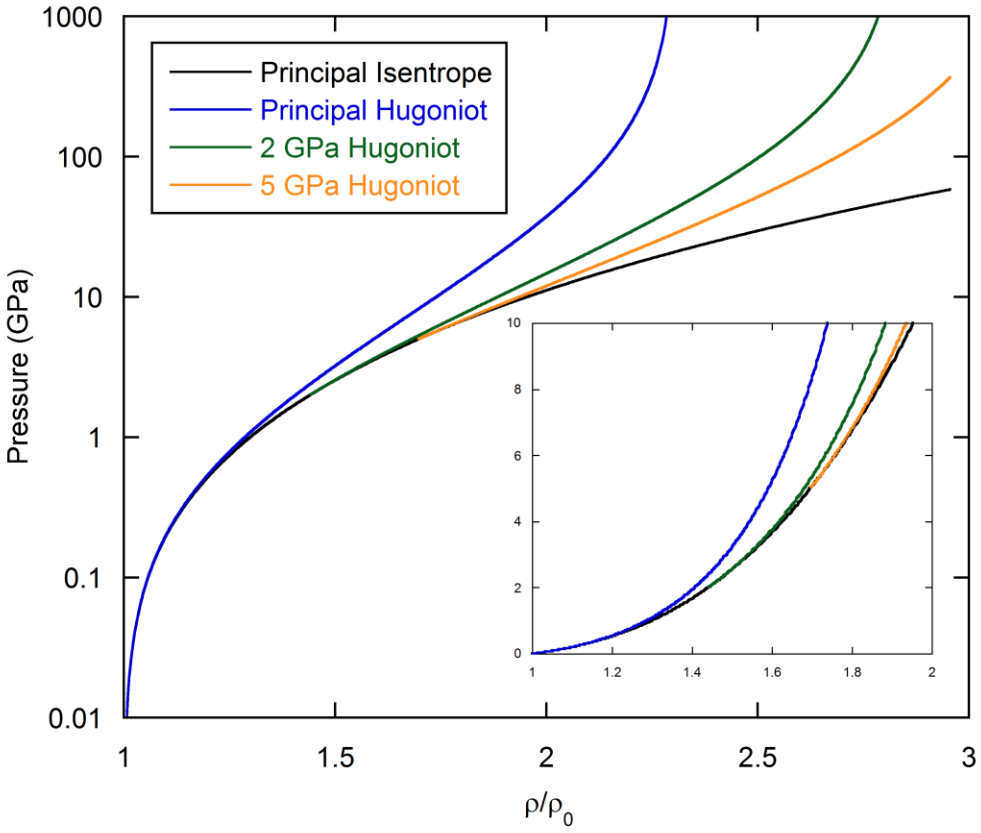

Figure 1. Principal Hugoniot, principal isentrope, and pre-compressed Hugoniots for neon, inset shows the same data on a linear scale.

Pre-compression is also the only method to study the shock response of homogeneous mixtures of hydrogen and helium. Helium condenses at 4 K and hydrogen at 20 K; however hydrogen solidifies at 14 K at ambient pressure. The difference in condensation and melting points prevents mixing a hydrogen-helium fluid at 1 bar. In addition, the H_2-He system exhibits a high degree of non-ideality manifested by a significant excess volume of mixing [8] and expansive miscibility gap [9] which is predicted to persist to multi-Mbar pressures [10]. Table 1 shows isopycnic properties of hydrogen and helium. It is possible to mix a homogeneous super-critical fluid mixture of hydrogen and helium at pressures greater than ~200 MPa and room temperature with densities close to those of the individual cryogenic liquids at 1 bar.

Table 1. Isopycnic *P*, *T* States of Hydrogen and Helium

Hydrogen at 0.8 g/cc	Helium at 0.15 g/cc
0.1 MPa, 14 K	0.1 MPa, 4 K
250 MPa, 298 K	150 MPa, 298 K

Hydrogen and helium are dominant components in stars and giant planets. The high pressure behavior of the mixture is critical to understanding the internal structure and thermal evolution of stellar objects. The ability to study the mixture under extreme conditions has the potential to open the window on significant physics affecting the internal structure of giant planets and stars. The demixing problem is not well understood, particularly under dynamic loading conditions. In addition, data on highly non-ideal mixtures such as hydrogen-helium would provide a good benchmark for theoretical mixing models at high pressure.

1.2. Techniques of Static Compression

Techniques of static compression were first developed in the early 20th century [11]. By modern static pressure technique standards, the pressures required for this project (100's MPa) are relatively low. Piston cylinder, multi-anvil, and diamond anvil cell techniques all routinely achieve stresses an order of magnitude greater or more [12]. However, the challenge of this project is in combining a large volume sample with geometry compatible with plate impact shock wave compression. Large volume high pressure techniques such as piston cylinder are too confining to be applicable as gas gun targets; and small volume diamond anvil cells have sub-millimeter samples much too small to be applicable. A diamond anvil cell type device is conducive to acting as a gun target if the sample dimensions could be increased by an order of magnitude while still maintaining a minimum 200 MPa pressure.

1.3. Project Overview

Techniques of dynamic compression utilizing shock waves are well established. Critical to obtaining accurate Hugoniot data is the avoidance of edge waves during shock transit through the sample. For pre-compressed targets, this requires thin anvils, thin samples, and "large" diameter samples. Various diamond anvil cell designs come close to meeting these criteria, with the major exception of large diameter. The biggest challenge of this LDRD was to develop a compression cell design which can support 100's MPa pressure on a sample at least 2.5 mm diameter. For comparison, typical diamond anvil cell samples have diameters on the order of 100 μm or less. It is also desirable to load gasses to above the critical point. Gasses are highly compressible, necessitating control or minimization of the sample diameter reduction during static compression. Ideally, most of the volume reduction will take place along the compression axis. In order to minimize sample diameter reduction from the sealing volume, gasses need to be sealed in the compression cell at high density. This is accomplished with a high pressure gas loading system described in Section 2.4.

Pre-compression targets were tested on the DICE gas gun in order to refine target design and the optical coating scheme utilized for diagnostics. Stress gradients in the anvils surrounding the target on the compression axis cause non-steady waves in the anvil, therefore absolute Hugoniot measurements by obtaining both particle and shock velocities and in-situ impedance matching standards are desirable. The best combination of diagnostics typically proved to be simultaneous VISAR and PDV. A subset of the dynamic tests conducted will be described in some detail.

2. PRE-COMPRESSION TARGETS

The goal of the LDRD in regards to target hardware was to develop a robust design which would have a high success rate of achieving 200 MPa pressure on the sample or higher. The cell should be compatible with various gas guns available at Sandia facilities (DICE and STAR) [13]. Diagnostic access was built into the design from the beginning, and alignment of the target to the gun barrel and diagnostics should be as simple as possible. The most appropriate diagnostics for these shots is velocimetry, both VISAR and PDV have been utilized. The reflective coating scheme was iterated upon in order to maximize the impact and data return on each shot. Considerable iteration on various design details were required to meet all objectives. With few exceptions, only the final design is detailed in the following sections.

2.1 Target Cell

Pre-compression hardware developed for this LDRD is based on the symmetric diamond anvil cell design [14]. The cell body is exposed to large stresses on static loading and therefore the piston and cylinder components are fabricated from 17-4 precipitation hardened (17-4 PH) steel. Hard steel should minimize deformation of the cell body during loading. The piston and cylinder are fabricated with a slip fit to ensure uniaxial loading when force is applied. Single crystal sapphire anvils oriented {100} and 2 mm thick are used to apply force to the sample. The anvils are 10 mm diameter at the girdle, 6 mm diameter at the culet, with a ~31 degree bevel. These anvils are supported with tungsten carbide (WC) seats. The piston and cylinder each have a uniquely designed seat. The piston thickness is 2 mm and the piston WC seat is also 2 mm thick in order to minimize the recess distance to the impact surface on the sapphire anvil. Anvils are secured to the WC seats with epoxy. The piston seat is held in place within the piston with 4 screws and is not adjustable. The cylinder seat position is adjusted within the cylinder using 4 set screws. The cylinder anvil position is adjusted to exactly mate with the piston anvil on contact. Four bolts fitted with Belleville washers are utilized to apply a force. On tightening the bolts, the Belleville washers compress transferring a uniaxial compression force to the anvil/sample stack. An exploded, annotated assembly drawing of the compression cell is shown in Figure 2.

The sample material is confined between the two sapphire anvils with gasketing. The gasket consists of three layers. A 0.5 mm thick indium disk with a 5 mm diameter through hole, a pre-fabricated copper gasket which matches the diameter and bevel of the anvils with a 5 mm diameter through hole, also 0.5 mm thick where it mates to the anvils, and finally another 0.5 mm thick indium disk with a 5 mm through hole. The total gasket stack thickness before compression is therefore 1.5 mm. The indium gasket was found to be necessary in addition to the copper to successfully seal a fluid in the sample chamber and increase pressure on the sample. Initial attempts at loading using only a copper gasket resulted in failed sealing and broken anvils. Presumably, the pre-fabricated copper gaskets did not perfectly mate to the shape of the anvils. As force was applied, the copper deformed and work hardened thus causing further deformation necessary for sealing to become increasingly difficult. At some point, the force required to deform the work hardened copper exceeded the force required to break the sapphire resulting in a failed load. Trial and error lead to the current indium-copper-indium design which has a nearly 100% sealing success rate.

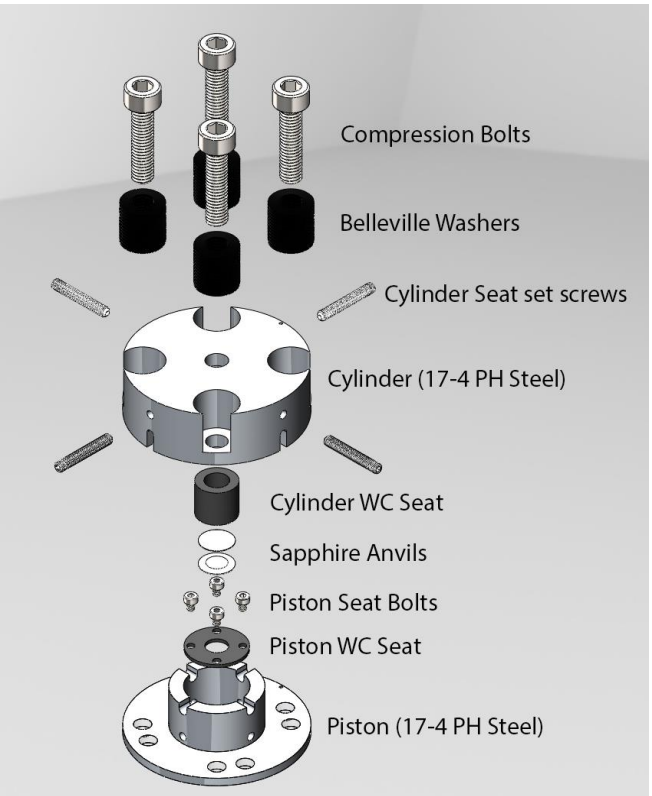

Figure 2. Pre-compression target cell design

The initially 1.5 mm thick composite gasket is reduced to 0.35-0.50 mm on compression to 200-500 MPa. Most of the gasket deformation and volume reduction occurs with the indium. In addition to thinning, the indium also creeps in towards the center of the anvils reducing the sample diameter from an initial 5 mm to 2.5-3 mm. On compressing the cell, one must carefully apply an equal force to each compression bolt to prevent asymmetric loading of the anvils which causes excessive deformation of the indium and typically failure to seal and/or anvil breakage. Symmetric loading was accomplished with a torque wrench and tightening each bolt sequentially by ½ inch-pound up to a maximum of 12 inch pounds. Exceeding the former torque typically resulted in broken anvils; however there was a large variation on the torque to force relation depending on number of and exact stacking scheme for the washers. Typical sample dimensions are shown in Table 2.

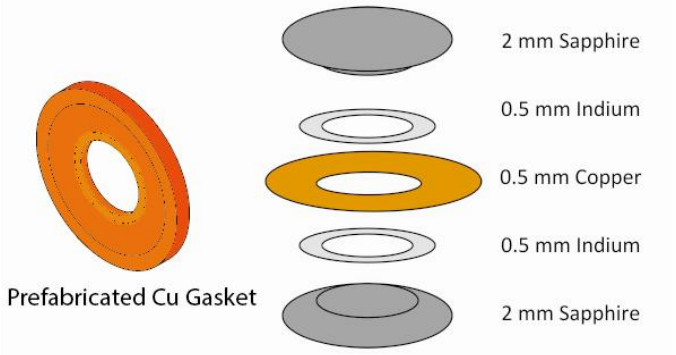

Figure 3. Gasketing scheme to hold sample between sapphire anvils.

Table 2. Typical Sample Dimensions

Anvil Thickness	2.0 mm
Anvil Diameter (at culet)	6.0 mm
Sample Thickness	0.3 – 0.5 mm
Sample Diameter	2.5 – 3.0 mm
Ruby Thickness	0.1 mm

Stress gradients will develop in the anvils and gasket during compression. The anvil and gasket surfaces in contact with the fluid sample will be at some high pressure and the free surfaces at ambient pressure. The most important of these gradients for the present project is the gradient along the compression axis. The sample is fluid and therefore does not support a pressure gradient; however radial gradients could pose a potential issue if one was inclined to pre-compress solid samples. A cartoon of the stress gradients present with a fluid sample assembly is shown in Figure 4. The axial gradient poses challenges for impedance matching with the anvil; waves that transit the anvil before breaking out into the fluid sample are unsteady as the traverse up a stress and density gradient.

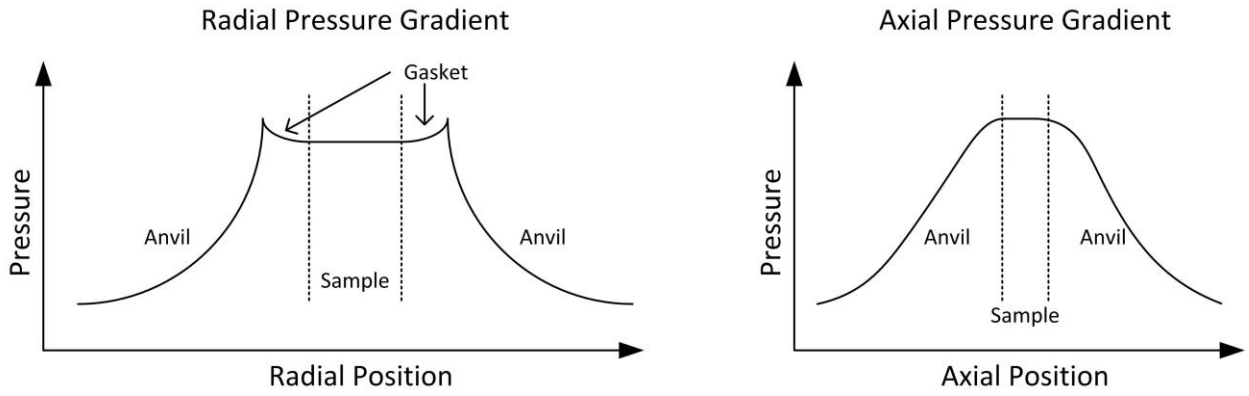

Figure 4. Pressure Gradients in the pre-compression cell

2.2 Pressure Measurement and Coating Scheme

Included in the sample stack is a 0.1 mm thick by 5 mm diameter disk of ruby (chromium doped aluminum oxide) which is glued directly to one of the sapphire anvils. Typical glue bond thicknesses were up to 40 μm on early tests, but improved substantially to 1-4 μm as experience and confidence with handling the sapphire/ruby was obtained. Ruby possesses a series of fluorescence lines in the red which are very sensitive to pressure and may be excited by yellow or shorter wavelength lasers [15]. A 561 nm, 100 mW laser was used for this project for lab testing and a 532 nm laser was used when targets where mounted in the gun target chambers. Ruby possesses two strong fluorescence lines in the red; the stronger of the two is the *R*1 line located at 694.24 nm at ambient conditions. The *R*1 line redshifts with increasing pressure by approximately 0.01 nm per 27 MPa. The accuracy of pressure measurement on the sample

therefore is directly related to the calibration of the ruby scale [16] and the resolution at which the *R*1 line position can be measured. With the ruby optical system built for this project, which is similar to previous designs [17], the resolution of the spectrometer is ~0.004 nm resulting in an estimated 10 MPa error on pressure measurement. Typical pre-compression pressures were 200-400 MPa, which corresponds to a 2.5 – 5 % error on pressure. Figure 4 shows a ruby spectrum at ambient pressure and a spectrum collected from a pre-compression assembly at 270 MPa.

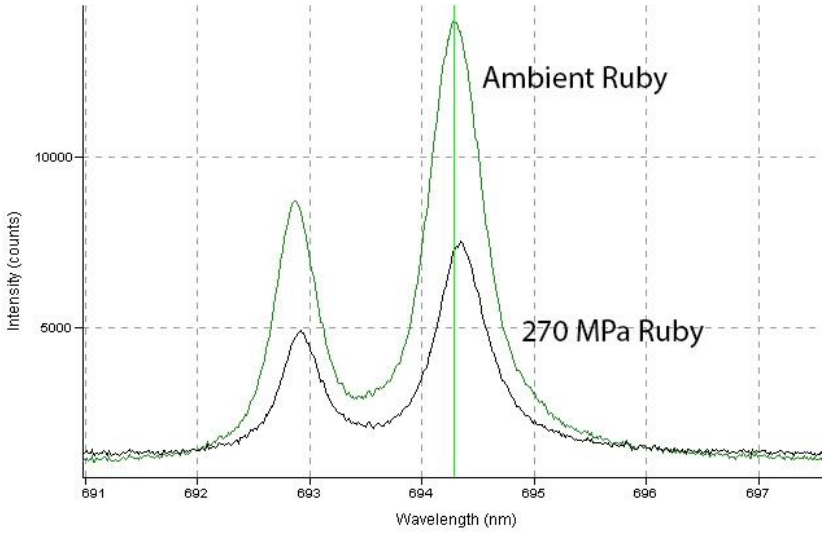

Figure 5. Ambient and high pressure fluorescence spectrum of ruby

Through the experience of building many targets, a practical pressure limit for the current design is ~450 MPa. Pressures of up to 1000 MPa or 1 GPa were achieved on a small number of samples, however the fluid diameters were less than 2.5 mm at these conditions and were not likely to produce high quality Hugoniot data. In addition, at pressures above 450 MPa the sapphire anvils were prone to cracking with immediate loss of pressure on the sample when this occurred. Therefore most targets that were prepared for dynamic testing were intentionally limited to below 450 MPa. Possible paths to improving the maximum pressure exist and are discussed in some detail within the conclusions section (Chapter 4).

Impedance matching with the sapphire anvils is difficult due to the stress gradients developed within them. Absolute Hugoniot measurements are therefore ideal when possible. A coating scheme was developed that allows a measurement of the particle velocity of the fluid and the shock transit time through the sample as long as the shocked fluid is transparent. The particle velocity and shock transit time along with the initial conditions of the sample and initial sample thickness allow an unambiguous determination of the Hugoniot state. Figure 6 shows a cartoon of the sample stack from the side with coatings pointed out. There is a spot coating of aluminum deposited onto the culet of the impact side anvil. The ruby which is glued to the cylinder/diagnostic side has a "donut" coating aligned with the spot coating. This donut coating is at the fluid/ruby interface. A record of wave arrival at the spot coating and donut coating provides a measure of shock transit time. A velocimetry record of the spot coating is the particle velocity of the fluid at the Hugoniot state. Should the shock wave become reflective, impedance matching with the ruby is in principle possible because it is at the same initial pressure and does not support measureable stress gradients.

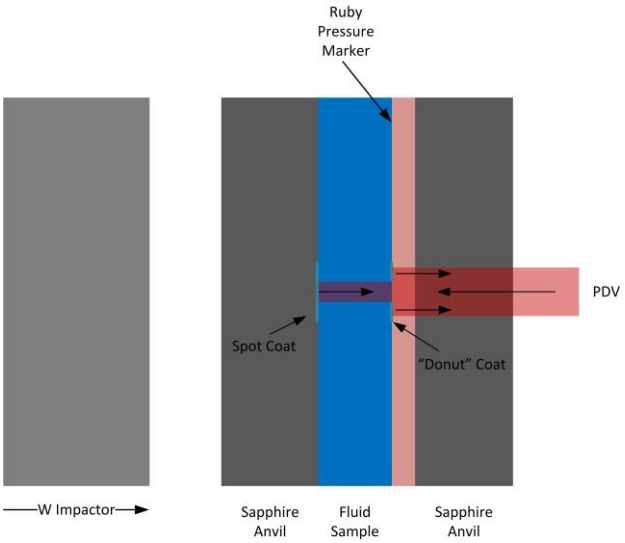

Figure 6. Side view of sample stack and coating scheme (not to scale)

A number of different diagnostic combinations were attempted on dynamic shots. Initially it was unknown if the target assembly would remain sealed and hold pressure while subject to the vacuum of a gun target chamber. For this reason, the initial diagnostic set-up included an open beam focusing VISAR system which could be intentionally misaligned to probe the ruby fluorescence during pump down. The system was designed such that the VISAR probe beam was focused onto the spot coat at the sapphire/fluid interface through the donut coating. This typically proved effective at returning particle velocities and often gave a shock transit time measurement. Loss of sample pressure was never observed on any target during pump down, indicating robust sealing of the fluid. Due to the complexities of an open beam focusing system, and the fact that targets were robust to pump down, fiber based diagnostics were applied for most of the later shots in the project. Fiber based VISAR and PDV were used to probe both reflectors and in some cases, probes were additionally fielded off-center to look for edge wave arrival times and the initial impact of the flyer. An image of a sample along the compression axis is shown in Figure 7 illuminated by a PDV collimated probe with a red laser. The donut coat can be seen in the left panel of Figure 7.

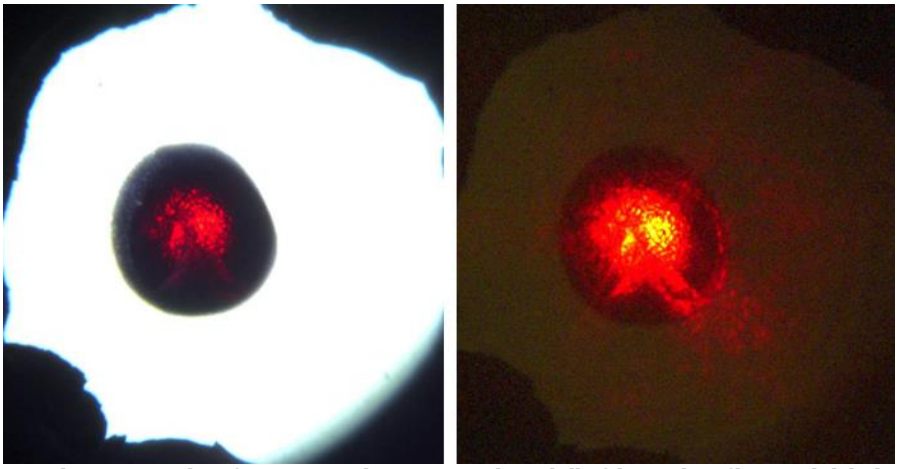

Figure 7. Photograph of a target in transmitted (left) and reflected (right) light.

Figure 8 shows photographs of targets for the DICE gas gun on the back (diagnostic) side (left), and the impact side (right). Note that the sapphire anvil impact surface is actually recessed 4 mm back from the flat of the target plate and bottom of the piston. The spot coating can be seen on the image of the impact surface. Shorting pins mounted to the target plate are used to measure projectile velocity and tilt of the projectile relative to the target plate. Gauge blocks and cylinders are utilized to ensure the impact surface of the sapphire anvil is parallel to the surface of the target plate. Figure 9 shows the target mounted in the DICE gas gun with the open beam focusing VISAR system.

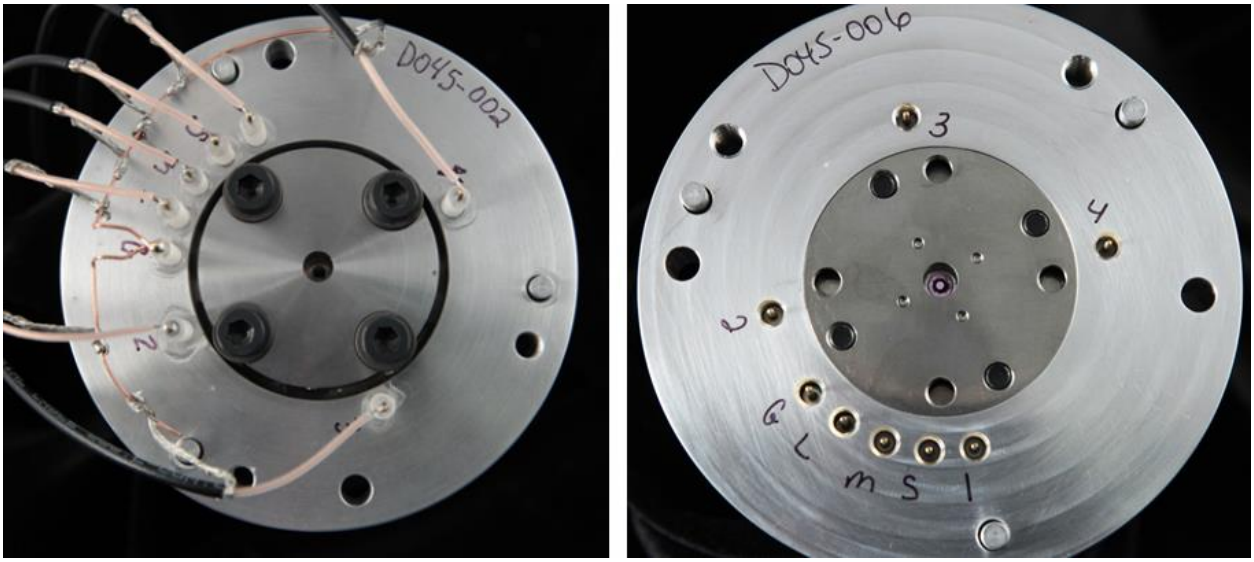

Figure 8. Photographs of the back side (left) and front/impact side (right) of a pre-compression target.

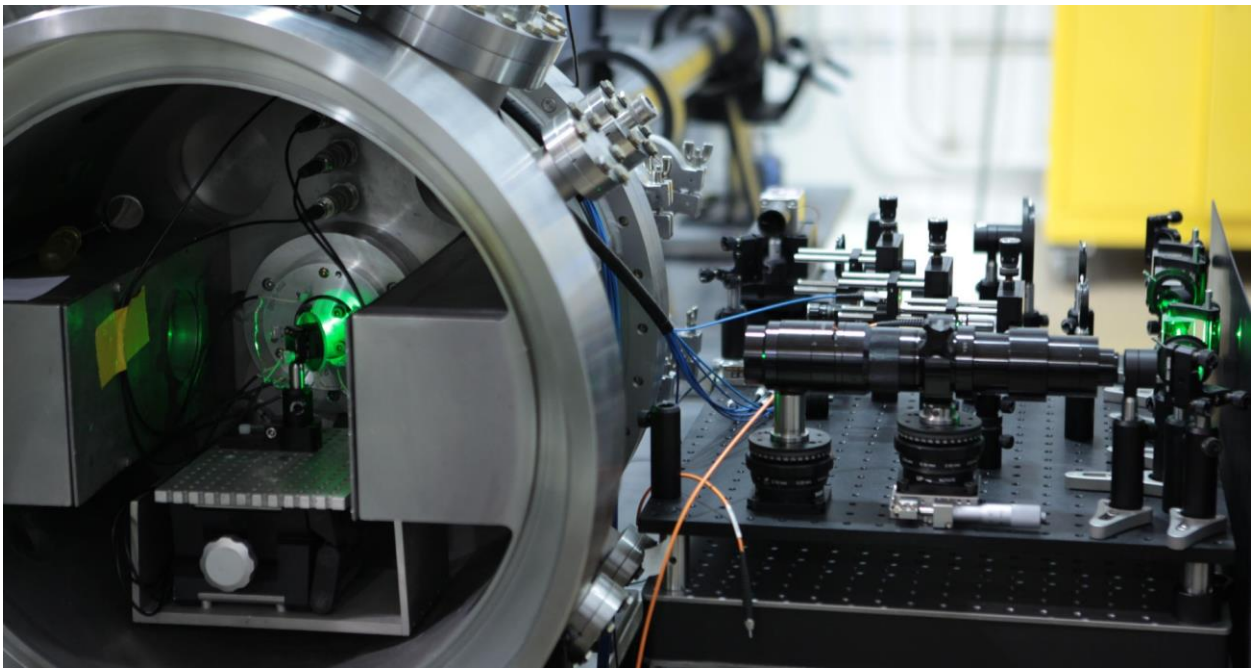

Figure 9. Target mounted on DICE gas gun with open beam VISAR diagnostic.

2.3 Projectile Design

As can be seen in on the right panel of Figure 9, the intended impact surface is recessed relative to the target plate front surface. The recession is approximately 4 mm for most targets built. The diameter of the recess is 6 mm, which matches the culet diameter of the sapphire anvils. The impactor is necessarily a smaller diameter than 6 mm as it must "thread the needle" without clipping the piston. The design chosen for DICE projectiles was a nose-piece that protrudes ~6 mm in front of the main body of the projectile. The aluminum nose piece is precision turned on a lathe such that the nipple is centered on the projectile. Aluminum was chosen to minimize mass of the projectile, however it is generally not the best choice for maximizing the dynamic pressure on the target. The design accommodates higher impedance impactors by gluing a 5.5 mm diameter impactor to the tip of the nosepiece. This was generally done for most of the DICE shots with tungsten or platinum impactors. Figure 10 shows one of the projectiles used on the DICE gun. A tungsten impactor can be seen glued to the aluminum nosepiece.

Figure 10. Projectile for DICE gas gun.

Alignment of the target to the gun barrel was accomplished with precision gauge pins which ensured centering of the target plate on the barrel. Despite the tight fit of the impactor (5.5 mm) in the recessed piston hole (6 mm), the impactor hit the target as intended on every dynamic test. This was evidenced by the data return and inspection of recovered hardware after the shots. Projectiles were launched up to 336 m/s at the DICE gun during this series of tests.

Projectiles for STAR shots necessitated a different design due to the much larger acceleration forces involved in launching on the 2-stage light gas gun. Instead of gluing on a nosepiece as in the DICE shots, a monolithic nosepiece was fabricated out of tantalum. This gave the impactor relatively higher strength to prevent disintegration before impact. The alignment procedure on the 2-stage light gas gun was also modified. A set of eight precision spacers were fabricated of identical thickness. A dummy projectile with the same dimensions as the real projectile was fabricated and placed in the gun barrel protruding slightly from the end in the target chamber. Four sets of two spacers were placed on screws between the target plate and the gun barrel. The target plate was then positioned exactly on the center of the dummy impactor and fixed in place. At this point, the spacers in contact with the target plate were glued to the target plate, and likewise those in contact with the barrel were glued to the barrel. The target was then removed, dummy projectile removed, and the target replaced on the barrel. The reproducibility of this procedure was tested and found to accurately position the target on the barrel in static testing. Figure 11 shows a STAR target and spacers mounted in the target chamber of the 2-stage light gas gun. Projectile velocities up to 4.6 km/s were tested with this configuration.

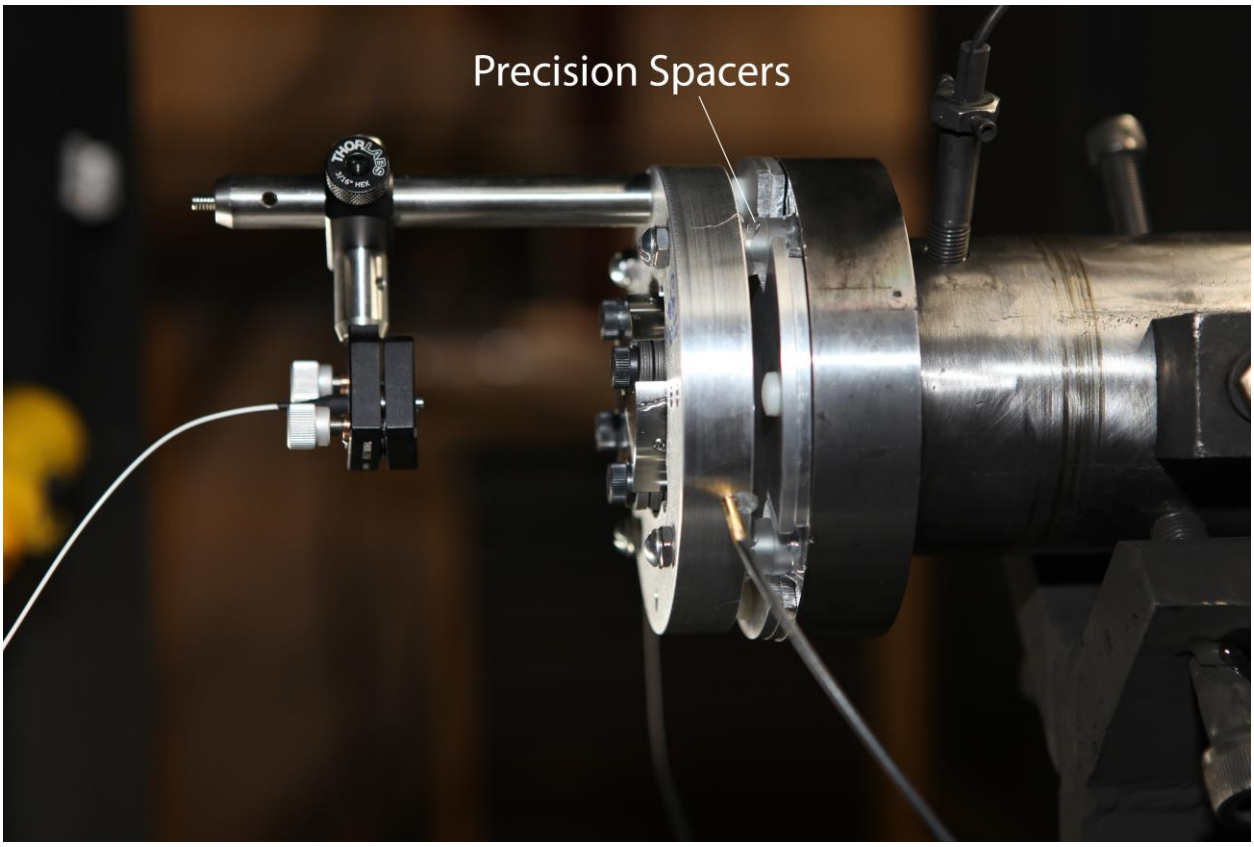

Figure 11. Pre-compression target mounted in the STAR 2SLGG target chamber.

2.4 Gas Loading

Prevention of sample volume collapse on compression must be controlled especially for highly compressible materials in order to obtain samples of large enough diameter to prevent edge

waves during dynamic testing. This is a particularly important issue for gas targets as volume collapses as high as 2000x relative to ambient conditions are possible. With this volume collapse there would be essentially no sample left at 200+ MPa if loaded at ambient pressure. Therefore, gas samples must be trapped in the compression cell at high pressure to begin with. This is accomplished with a high pressure gas loader with a working pressure of 25,000 psi (172 MPa) [18]. A diagram of the system is shown in Figure 12.

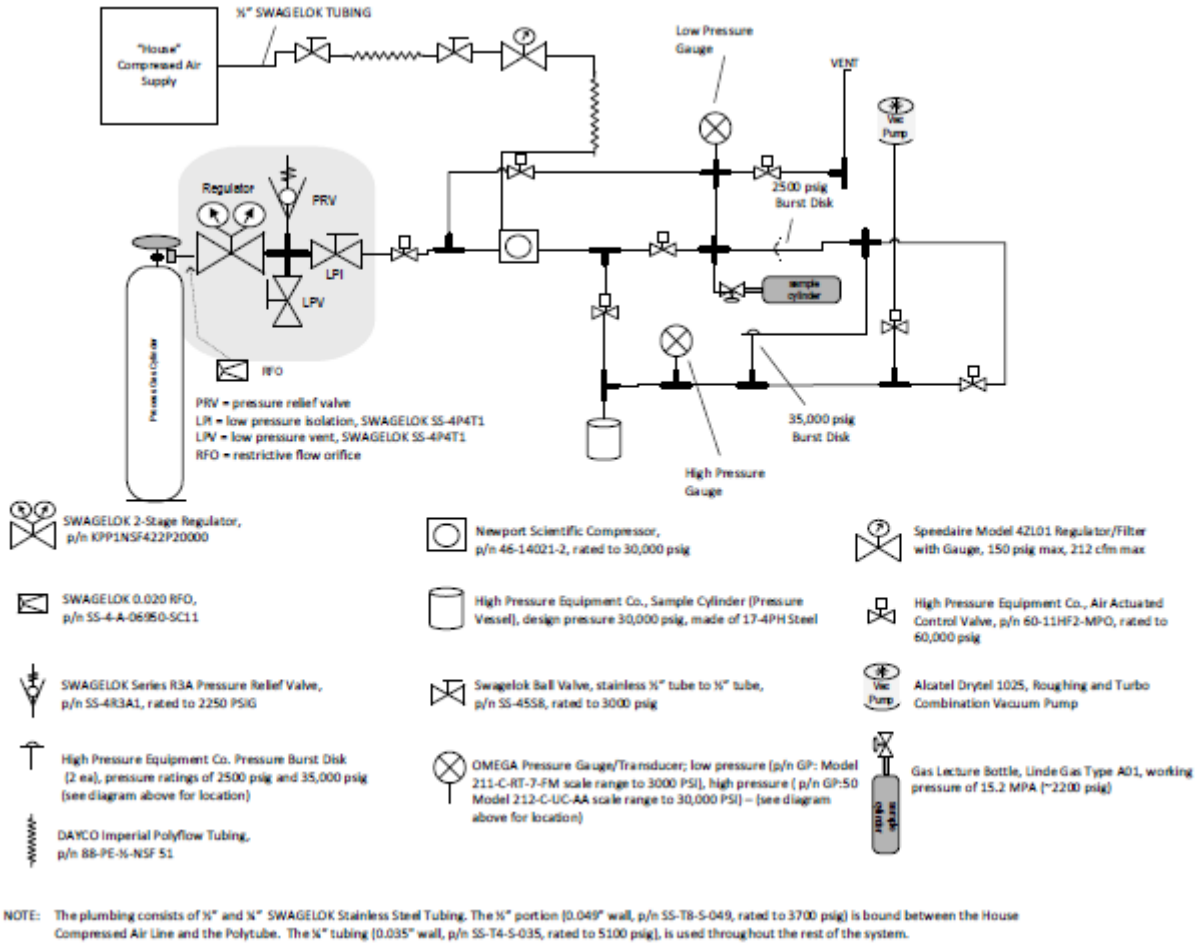

Figure 12. Diagram of the high pressure gas loading system

The pre-compression cell is pressurized in the open position within a pressure vessel. An optical sapphire window allows diagnostic access to the cell during the pressurization and sealing process. The pressure on the vessel is monitored with transducers and the pressure on the sample itself is optically monitored with ruby fluorescence through the window. The pre-compression cell sits in a bolt driven clamping mechanism within the pressure vessel. Rotary feed throughs into the pressure vessel drive an elevator on the clamping mechanism up, effectively applying a compression force to the piston and cylinder. This force is applied once the pressure vessel is at 172 MPa. As force is increased on the piston/cylinder with the clamping mechanism the pressure on the sample increases beyond 172 MPa up to 200-300 MPa. This ensures that the sample gas is sealed within the cell. The pressure vessel is then vented, clamping mechanism removed, and the Belleville washer bolts are then tightened up to 6-12 inch-lbs to transfer the load from the

clamping mechanism to the washers. The target can then be removed from the clamping mechanism and inspected. A pressure measurement on the target with ruby fluorescence once removed is used to verify the gas is sealed within the target. Figure 13 shows an annotated image of the gas loading system including the pressure vessel (left) and high pressure plumbing (right).

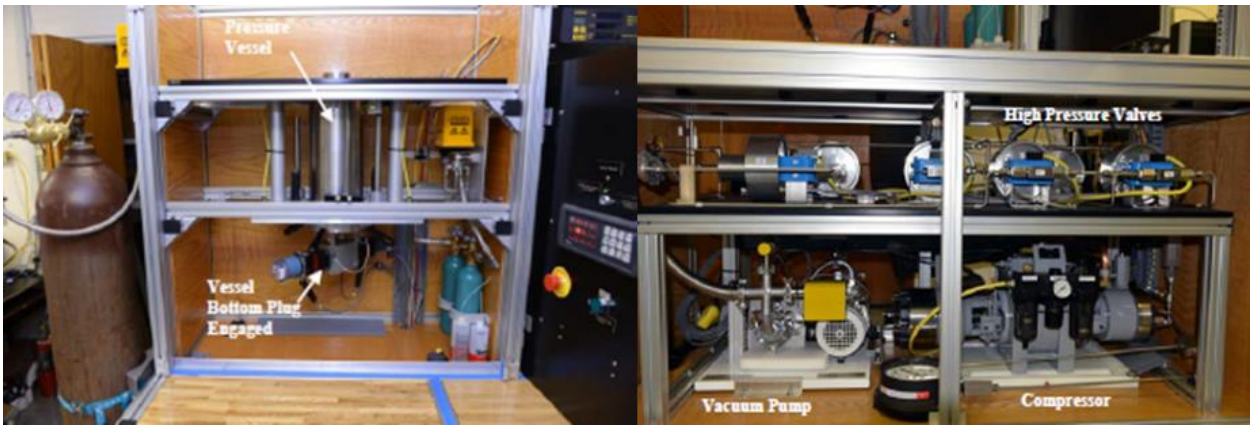

Figure 13. Annotated image of the gas loading system.

3. DYNAMIC LOADING OF PRE-COMPRESSED TARGETS

Initial dynamic testing on the DICE gas gun focused on the development of diagnostics for these targets and verification that impactors were correctly impacting the intended area of the target. The first DICE shot confirmed the former. Later tests focused on the refinement of diagnostics and the collection of pre-compressed Hugoniot data on ethanol. Ethanol was chosen because it was readily available, easy to load in the pre-compression cell and principal Hugoniot [19, 20] and principal isotherm [21, 22] data are available. Parallel to this dynamic testing was the set-up and testing of the gas loading system described in the previous section.

Three tests on the STAR 2-stage light gas gun were conducted on pre-compressed helium samples. It was discovered diagnostic probe design again had to be modified for these shots due to the more violent nature of pre-impact vibrations. The third test at STAR successfully returned good data. This chapter describes a subset of executed shots, analysis, and results of the data obtained to date.

3.1 Dynamic Loading of Pre-Compressed Ethanol

A total of six dynamic experiments on ethanol pre-compressed to pressures between 100 and 350 MPa returned data of sufficient quality to extract Hugoniot data. The isothermal compression data from Brown et al. [22] was utilized to determine the initial density of the samples in combination with the ruby fluorescence pressure measurement. Velocimetry traces from shots PC_2 and PC_3 on the DICE gas gun are presented in Figure 14 along with simulations of the experiments. It should be noted that these one dimensional hydrocode simulations of the experiment do not include pre-compression. Pre-compression is treated as unsupported in the codes and on initialization of a pre-compression target, an initial pressure above zero will immediately begin to relax by launching release waves into surrounding material. This is a short coming of the available hydrocodes which may need to be remediated if a significant number of additional experiments are planned for the future.

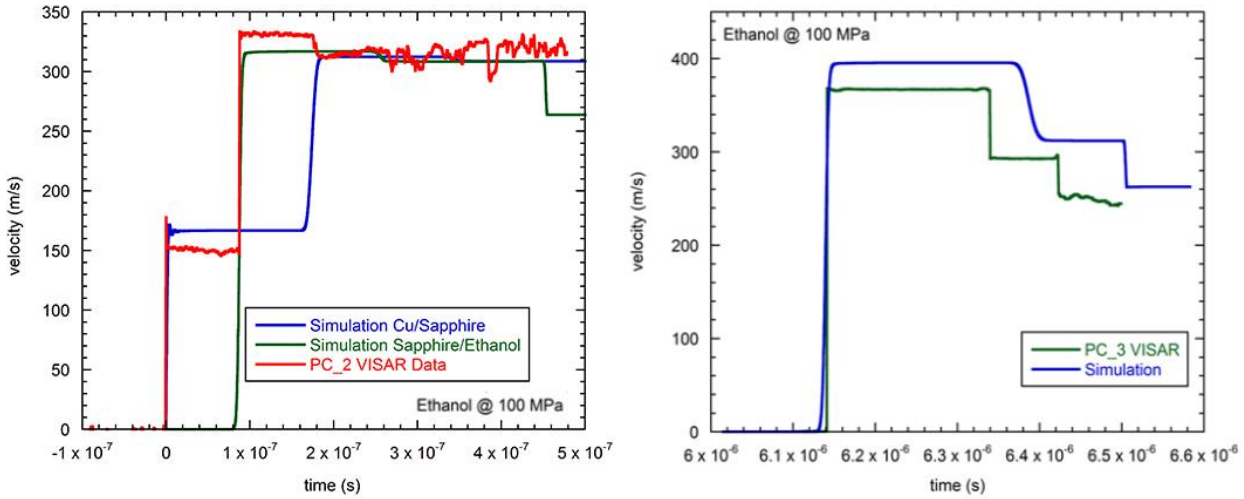

Figure 14. Velocimetry and simulations for DICE shots PC_2 and PC_3. The simulations do not include pre-compression.

DICE shot PC_2 had a tungsten projectile velocity of 328 m/s. This target hardware had no reflective coatings. Shot PC_3 also had a tungsten projectile launched at a velocity of 332 m/s. This target had a single reflective coating at the sapphire/ethanol interface and VISAR successfully recorded the particle velocity. Shot PC_5 was pre-compressed to 350 MPa and also utilized a tungsten projectile at 330 m/s. On this particular shot, the ruby was bonded to the front (impact side) anvil with nearly 40 µm of glue. This caused ringing in the particle velocity at the ruby/ethanol interface, however it was still possible to analyze this data by taking an average of the velocity over the "steady" time period before reverberation. A velocity record of this shot is shown in Figure 15.

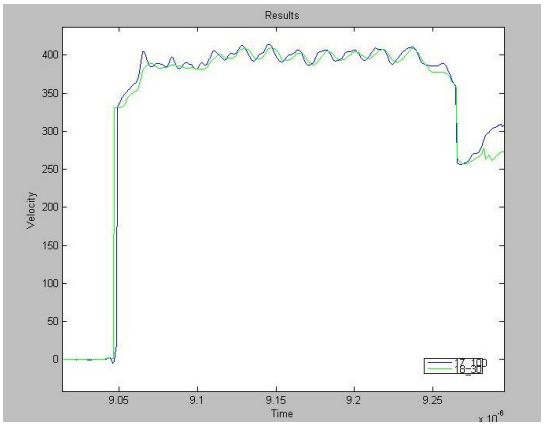

Figure 15. VISAR velocity record for shot PC_5 showing records from two different sensitivities.

A single fiber PDV probe was utilized in addition to VISAR on shot PC_11 which utilized a tungsten impactor at a velocity of 336 m/s. This target was in the final configuration as described in Chapter 2, with both the spot and donut coatings. The PDV was able to record the impact on the sapphire, particle velocity of the sapphire/ethanol interface and the shock transit time through the fluid sample. A spectrogram of the PDV record is shown in Figure 16. VISAR was also fielded on this shot looking at the spot coating at the sapphire/ethanol interface. It was found to match the velocity determined from the PDV data, providing confidence in using a single PDV fiber for future STAR shots. Also, as seen on Figure 16, the PDV sees the velocity and shock break-out times of all interfaces of interest further supporting the switch to a simpler probe design.

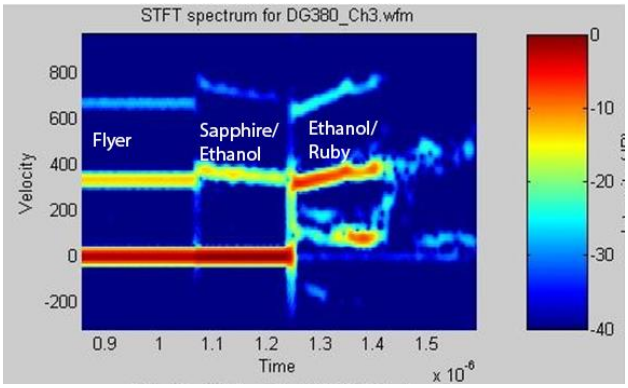

Figure 16. PDV spectrogram velocity record of shot PC_11.

An analysis of the available shots is compared to the principal Hugoniot and principal isotherm in Figure 17. Errors are quite large due in part to the sparse data on the isotherm in the 100's MPa range; the EoS in this region is used to constrain the initial density of the sample. The pre-compressed Hugoniot lines in Figure 17 are calculated based on the principal Hugoniot and isotherm. The data set is generally consistent with expectations; the data at higher pre-compressions are experimentally distinguishable from the principal Hugoniot.

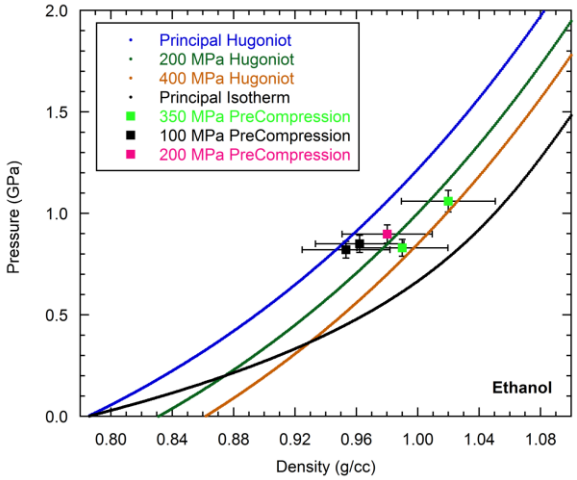

Figure 17. Pre-compressed Hugoniot data for Ethanol compared to the principal Hugoniot and isentrope.

3.2 Dynamic Loading of Pre-Compressed Helium

Three shots were executed at STAR in Sept. 2015. The success of the single fiber send/return PDV in the latest DICE shots lead us to drop the VISAR on the first two shots to simplify the alignment of the diagnostics. Unfortunately, data return was poor on both of these shots likely due to tilt on impact and/or mis-alignment of the PDV fiber occurring during the early stages of the gun firing, well before the projectile reached the target. Sound waves generated by the explosive charge in the breech outrun the projectile and vibrate the target hundreds of microseconds before the projectile reaches the target. On both of these first shots, the PDV fiber diagnostic was mounted on a, in retrospect, lever arm as seen in Figure 11. For a third shot, a "Romulan" probe was used which consists of four 200 µm core multi-mode fibers (for VISAR) and three 9 µm core single mode fibers (for PDV) all positioned in a single hypo. The probes were mounted ~1 mm from the free surface of the cylinder sapphire anvil pointed and at the donut and spot coats. Both the PDV and VISAR were configured for separate send/receive fibers which should greatly reduce probe sensitivity to tilt of the impactor. The probe was also glued directly to the cylinder of the pre-compression cell in an attempt to mitigate relative vibrations of the probe and target. The sample consisted of a 270 MPa pre-compressed helium sample (Figure 5 shows the ruby spectrum of this sample). Isothermal fluid data at room temperature [23] was used to constrain the initial density of the sample, 0.21 g/cc. Figure 18 shows the PDV spectrogram velocity records from this shot. This shot utilized a tantalum impactor with a velocity of 4.56 km/s.

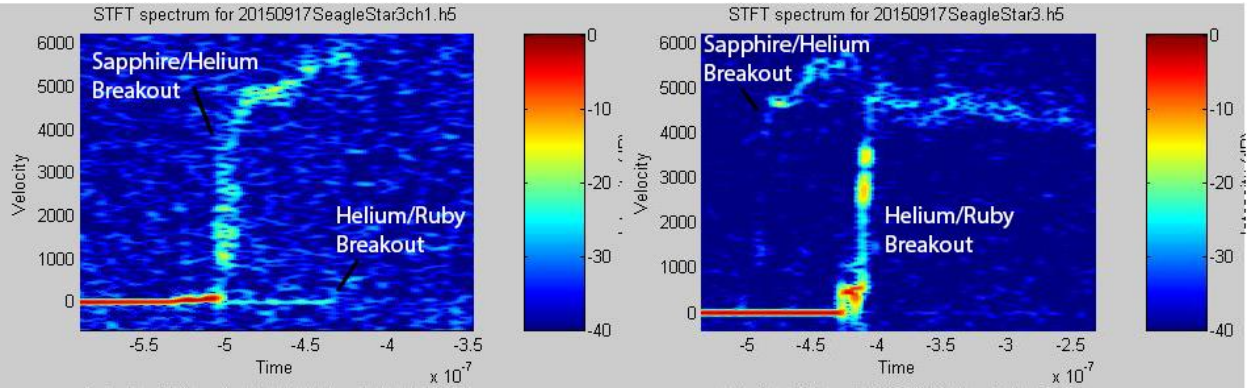

Figure 18. PDV velocity spectrogram from two channels on shot STAR_3.

A full analysis of this shot has not been completed as the data was collected on the last day of FY15, however a preliminary analysis of the data suggests a shock velocity of 6.9 km/s and a particle velocity of 4.66 km/s. The resulting pressure/density state (7.0 GPa and 0.65 g/cc) on the pre-compressed Hugoniot is compared to available cryogenic Hugoniot data [24] and room temperature compression data [23] in Figure 19. The solid lines on the figure are model calculations utilizing a fit to the room temperature isothermal compression data and the Hugoniot relation with a volume dependent Grüneisen parameter ($\gamma = \gamma_0(V/V_0)^q$), with $\gamma_0 = 1.6$ and $q = 0.55$. Laser shock data are available for pre-compressed helium at much higher pressures [25], making a direct comparison here difficult.

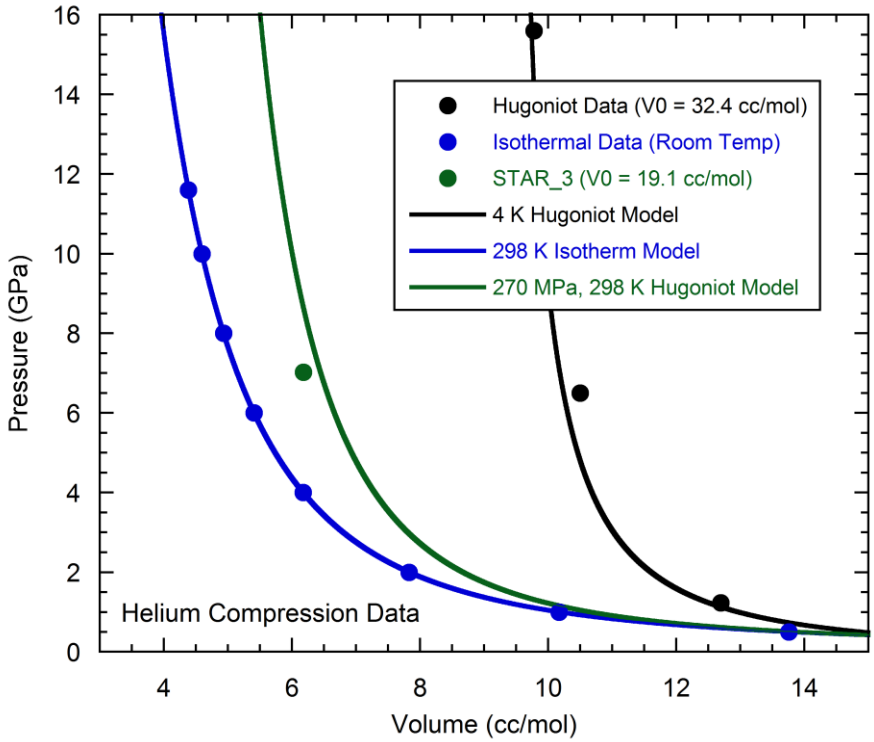

Figure 19. Helium Compression data.

4. CONCLUSIONS AND FUTURE WORK

A pre-compression target design was developed for use with gas guns for plate impact type Hugoniot studies. The pre-compression hardware is routinely capable of achieving 450 MPa, higher pressures are possible but challenging. Static pressures are measured with a ruby fluorescence marker in the sample stack. Samples are large enough to avoid edge waves and maintain uniaxial compression over the course of a dynamic experiment in most cases.

Gasses may be sealed in the pre-compression cell at 25,000 PSI using a gas loading system. This prevents collapse of the sample volume on compression. The gas loading system is capable of loading mixed gasses such as hydrogen-helium mixtures, but is currently limited to non-flammable mixtures (<8.7 mol % H). Low initial sealing success rates with the system (~20%) have improved substantially with experience using the system; 100 % sealing success for the last 6 targets produced, including 5 helium targets and one 8 wt. % hydrogen in helium target.

Several dynamic tests on DICE were executed with pre-compressed ethanol samples. Initial concerns with sample leakage on pumpdown and projectile misalignment clipping the piston were unfounded. Targets were robust and projectiles never missed the intended target. Early tests utilizing only VISAR often provided a particle velocity but failed to provide a clear indication of the shock transit time. A combination of VISAR and PDV used on later tests typically provided all necessary information for absolute Hugoniot measurements.

Three tests on the 2-stage light gas gun at the STAR facility were executed with pre-compressed helium samples. The higher velocities involved proved more challenging. The first shot likely suffered from tilt, the second shot had the diagnostic become misaligned at least 70 μs before impact likely resulting from sound waves in the barrel generated by the explosive charge. The probe design was modified for the third test to a more robust-to-tilt configuration with separate send and receive probes. Both VISAR and PDV probes were hard mounted and glued directly to the cylinder of the pre-compression cell. This shot returned good data.

Additional tests on the 2-stage gun are required to validate the diagnostic design. If proven to have a high success rate, tests utilizing the Z Machine with significantly higher impact velocities could provide interesting data. Development work could be undertaken to increase the maximum static pressure on the targets. Several viable options exist including utilizing single crystal diamond anvils instead of sapphire; this would significantly increase the cost however. Modifying the shape of the anvils and the tungsten carbide seats to increase the supporting forces on the anvils could also improve the maximum achievable pressure. The gas loading system needs to be certified for use with flammable gasses. Only minor modifications are likely needed to the system to support this function. Most critical to future development is continued support for this research. It represents the presently only viable route to obtaining high accuracy shock compression data on hydrogen-helium mixtures.

5. REFERENCES

1. Medvedev, A.B. and R.F. Trunin, Shock compression of porous metals and silicates. *Physics - Uspekhi*, 2012. **55**(8).
2. Duffy, T.S. and T.J. Ahrens, Free surface velocity profiles in molybdenum shock compressed at 1400 C, in *High-Pressure Science and Technology*, S.C. Schmidt, et al., Editors. 1993, Amer. Inst. Phys.: NY. p. 1079.
3. Knudson, M.D., J.R. Asay, and C. Deeney, Adiabatic release measurements in aluminum from 240 to 500 GPa states on the principal Hugoniot. *J. Appl. Phys.*, 2005. **97**: p. 073514.
4. Knudson, M.D., et al., Principal Hugoniot, reverberating wave, and mechanical reshock measurements of liquid deuterium to 400 GPa using plate impact techniques. *Phys. Rev. B*, 2004. **69**: p. 144209.
5. Davis, J.-P., Experimental measurement of the principal isentrope for aluminum 6061-T6 to 240 GPa. *J. Appl. Phys.*, 2006. **99**: p. 103512.
6. Seagle, C.T., et al., Shock-ramp compression: Ramp compression of shock-melted tin. *Appl. Phys. Lett.*, 2013. **102**: p. 244104.
7. Jeanloz, R., et al., High-Pressure Geoscience Special Feature: Achieving high-density states through shock-wave loading of precompressed samples. *Proc. Nat. Acad. Sci. USA*, 2007. **104**: p. 9172.
8. Sneed, C.M., R.E. Sonntag, and G.J. Van Wylen, Helium-Hydrogen liquid-vapor equilibrium to 100 atm. *J. Chem. Phys.*, 1968. **49**: p. 2410.
9. Street, W.B., Phase equilibria in molecular hydrogen-helium mixtures at high pressure. *Astrophys. J.* , 1973. **186**: p. 1107.
10. Lorenzen, W., B. Holst, and R. Redmer, Demixing of hydrogen and helium at megabar pressures. *Phys. Rev. Lett.*, 2009. **102**: p. 115701.
11. Bridgman, P.W., The measurement of hydrostatic pressures up to 20,000 kilograms per square centimeter. *Proc. Am. Acad. Arts Sci.*, 1911. **47**: p. 321.
12. Ito, E., Theory and Practice - Multianvil cells and High-Pressure Experimental Methods, in *Treatise on Geophysics*, G. Shubert, Editor 2007, Elsevier: Amsterdam. p. 198.
13. Asay, J.R., The Sandia National Laboratories Shock Thermodynamics Applied Research (STAR) Facility. *Sandia Report*, 1981. **SAND81-1901**.
14. Mao, H.-K. and W.L. Mao, Theory and Practice - Diamond-Anvil cells and probes for high *P-T* Mineral Physics Studies, in *Treatise on Geophysics*, G. Shubert, Editor 2007, Elsevier: Amsterdam. p. 231.
15. Eggert, J.H., K.A. Goettel, and I.F. Silvera, Ruby at high pressure. I. Optical line shifts to 156 GPa. *Phys. Rev. B*, 1989. **40**: p. 5724.
16. Chijioke, A.D., et al., The ruby pressure standard to 150 GPa. *J. Appl. Phys.*, 2005. **98**: p. 114905.
17. Barnett, J.D., S. Block, and G.J. Piermarini, An optical fluorescence system for quantitative pressure measurement in the diamond anvil cell. *Rev. Sci. Instrum.*, 1973. **44**: p. 1.
18. Rivers, M., et al., The COMPRES/GSECARS gas-loading system for diamond anvil cells at the Advanced Photon Source. *High Press. Res.*, 2008. **28**: p. 273.
19. Ahrens, T.J. and M.H. Ruderman, Immersed-Foil method for measureing shock wave profiles in solids. *J. Appl. Phys.*, 1966. **37**: p. 4758.

20. Petersen, C.F. and J.T. Rosenberg, Index of refraction of ethanol and glycerol under shock. *J. Appl. Phys.*, 1969. **40**: p. 3044.
21. Gromnitskaya, E.L., et al., Hydrogen-bonded substances under high pressure: Ultrasonic study of the low temperature phase diagrams of methanol, ethanol, and H_2O ice. *Joint 20th AIRAPT - 43rd EHPRG, June 27 - July 1, Germany*, 2005.
22. Brown, J.M., et al., Velocity of sound and equations of state for methanol and ethanol in a diamond-anvil cell. *Science*, 1988. **241**: p. 65.
23. Le Toullec, R., P. Loubeyre, and J.-P. Pinceaux, Refractive-index measurements of dense helium up to 16 GPa at *T*=298 K: Analysis of its thermodynamic and electronic properties. *Phys. Rev. B*, 1989. **50**: p. 2368.
24. Nellis, W.J., et al., Shock compression of liquid helium to 56 GPa (560 kbar). *Phys. Rev. Lett.*, 1984. **53**: p. 1248.
25. Eggert, J.H., et al., Shock experiments on pre-compressed fluid helium. *AIP Conf. Proc.*, 2009. **1161**: p. 26.

DISTRIBUTION

1	MS0344	A.J. Lopez	2624
1	MS1106	T. Ao	1646
1	MS1189	J.F. Benage	1646
1	MS1189	J.-P. Davis	1646
1	MS1189	M.P. Desjarlais	1600
1	MS1189	D.H. Dolan	1646
1	MS1189	T. Mattsson	1641
1	MS1189	S. Root	1646
1	MS1189	C.T. Seagle	1646
1	MS1189	P.E. Specht	1646
1	MS1193	R.G. Hacking	16561
1	MS1193	S. Payne	16561
1	MS1195	S.C. Alexander	1646
1	MS1195	J. Brown	1646
1	MS1195	D. Flicker	1640
1	MS1195	M.D. Furnish	1646
1	MS1195	R.J. Hickman	1647
1	MS1195	M.D. Knudson	1646
1	MS1195	G.T. Leifeste	1647
1	MS1195	W.D. Reinhart	1647
1	MS1195	J. Wise	1646
1	MS9042	T.J. Vogler	8256
1	MS0899	Technical Library	9536 (electronic copy)
1	MS0359	D. Chavez, LDRD Office	1911


Sandia National Laboratories